Biochemical and Biophysical Research Communications 452 (2014) 1028–1033

Contents lists available at ScienceDirect

Biochemical and Biophysical Research Communications

journal homepage: www.elsevier.com/locate/ybbrc

Quercetin suppresses insulin receptor signaling through inhibition of the insulin ligand–receptor binding and therefore impairs cancer cell proliferation

Feng Wang [a,b], Yong Yang [b,c,*]

[a] Department of Gastroenterology, The Tenth People's Hospital of Shanghai, Tongji University, Shanghai 200072, People's Republic of China
[b] Department of Nanomedicine, Houston Methodist Research Institute, Houston, TX 77030, USA
[c] Department of Medicine, Weill Cornell Medical College, New York, NY 10065, USA

ARTICLE INFO

Article history:
Received 4 September 2014
Available online 18 September 2014

Keywords:
Quercetin
Insulin receptor signaling
Single-molecule imaging
Single-molecule force measurement
Cancer therapy

ABSTRACT

Although the flavonoid quercetin is known to inhibit activation of insulin receptor signaling, the inhibitory mechanism is largely unknown. In this study, we demonstrate that quercetin suppresses insulin induced dimerization of the insulin receptor (IR) through interfering with ligand–receptor interactions, which reduces the phosphorylation of IR and Akt. This inhibitory effect further inhibits insulin stimulated glucose uptake due to decreased cell membrane translocation of glucose transporter 4 (GLUT4), resulting in impaired cancer cell proliferation. The effect of quercetin in inhibiting tumor growth was also evident in an *in vivo* model, indicating a potential future application for quercetin in the treatment of cancers.

1. Introduction

Insulin receptor signaling plays a crucial role in a diverse range of biological activities, such as cell growth, differentiation, apoptosis, and biological aging process [1–3]. Deregulation of this signaling pathway has been implicated in the pathogenesis of many diseases including cancer [4]. For example, upregulation of insulin receptor (IR) often promotes cancer cell proliferation [5,6]. Therefore, developing insulin receptor signaling inhibitors not only facilitates the control of biological processes for cell biology study, but also becomes an attractive way to develop new therapeutic reagents and anticancer drugs [7].

Insulin signaling is initiated by the ligand binding to IR, which induces IR to form a homodimer signaling complex on cell membrane. This leads to the phosphorylation of IR and then the phosphorylation of intracellular insulin receptor substrate 1 (IRS-1), to propagate the signal transduction [8–10]. Previous reports have shown that quercetin, a natural predominant flavonoid with many pharmacological activities, is able to inhibit the phosphorylation of IR in the presence of insulin [11]. However, the molecular mechanism on the inhibitory effect remains poorly understood. In this study, we used two single-molecule techniques, single-molecule force spectroscopy and single-molecule fluorescence microscopy to investigate its inhibition mechanism. Both single-molecule force spectroscopy and single-molecule fluorescence microscopy are emerging techniques to detect the initial cell signaling events on the live-cell membrane, which are difficult to investigate by the conventional biochemical assays with cell lysates and ensemble averaging [12]. We also demonstrate that quercetin as a novel small-molecule inhibitor of insulin receptor signaling can be used for cancer therapy.

2. Materials and methods

2.1. Cell culture and transfection

MDA-MB-231 cells were cultured with Dulbecco Modified Eagle Medium (DMEM) (Gibco) supplemented with 10% fetal bovine serum (FBS) (HyClone). The DNA fragment encoding full-length insulin receptor (IR) was subcloned into the HindIII and BamHI sites of pEGFP-N1 (Clontech), yielding the IR-GFP expression plasmid. Transfection of IR-GFP plasmid was performed using lipofectamine 2000 (invitrogen). Cells growing in a 35-mm glass-bottom dish (MatTek) were transfected with 0.4 μg/mL plasmids in the phenol red-free DMEM. To achieve a low-level protein expression, cells were incubated with the plasmid for 5 h, washed, and then imaged in the phenol red-free DMEM under the fluorescence microscopy. For quercetin treatment, the transfected cells which

* Corresponding author at: Department of Nanomedicine, Houston Methodist Research Institute, Houston, TX 77030, USA.
E-mail address: yyang@houstonmethodist.org (Y. Yang).

http://dx.doi.org/10.1016/j.bbrc.2014.09.039
0006-291X/

were ready for single-molecule imaging were incubated with 100 μM quercetin (Sigma) in the serum-free DMEM for 1 h at 37 °C before fluorescence imaging. For insulin stimulation experiment, the transfected cells were incubated with 100 nM insulin (Roche Diagnostics) in the serum-free DMEM for 30 min at 37 °C.

2.2. Atomic force microscopy (AFM)

Preparations of chemical modification of AFM tips (type: NP, from Veeco, Santa Barbara, CA, USA) and extracellular domain of IR (IR-ECD) were carried out as previously reported [13,14]. The force measurements of the insulin-modified AFM tip on the living MDA-MB-231 cells were carried out on a PicoSPM II with PicoScan 3000 controller and a large scanner (Molecular Imaging, Tempe, AZ). The AFM scanner was mounted on an inverted fluorescence microscopy (Olympus IX81, Japan). The loading rate of Force measurements was 1.0×10^4 pN/s. The force curves measured in living MDA-MB-231 cells were recorded and analyzed by PicoScan 5 software (Molecular Imaging, Tempe, AZ). All forces were measured with contact mode at room temperature. Cells were treated with vehicle (0.1% dimethyl sulfoxide (DMSO)) or quercetin (100 μM) or the extracellular domain of IR for 1 h.

2.3. Flow cytometry

Flow cytometry was used to measure the binding of insulin to IR. MDA-MB-231 cells were incubated with vehicle (0.1% DMSO) or quercetin (100 μM), in the presence of biotinylated insulin (Biocompare) for 1 h. Then the cells with biotinylated insulin were incubated with avidin-FITC (Invitrogen) for 30 min.

2.4. Single-molecule fluorescence microscopy

Single-molecule fluorescence imaging was performed with the objective-type total internal reflection fluorescence microscopy using an inverted microscope (IX 81, Olympus, Japan), a total internal reflective fluorescence illuminator, a 100X/1.45NA Plan Apochromat TIR objective (Olympus, Japan) and a 14-bit back-illuminated electron-multiplying charge-coupled device (EMCCD) (Andor iXon DU-897 BV). The microscope was equipped with a CO_2 incubation system (INU-ZIL-F1, TOKAI HIT) and live cell imaging was performed at 37 °C in 5% CO_2. GFP was excited at 488-nM by an argon laser (Melles Griot, Carlsbad, CA) with the power of 5 mW measured after the laser passing through the objective in the epi-fluorescence mode. The collected fluorescent signals were passed through two filters, BA510IF and HQ 525/50 (Chroma Technology), before directed to the EMCCD. The gain of EMCCD was set at 300. Only the central quarter of the chip (256 × 256 pixels) was used for imaging analysis to ensure homogeneous illumination. Movies of 200 frames were acquired for each sample at a frame rate of 10 Hz using MetaMorph software (Molecular Device). For the photobleaching-step counting study, before the single-molecule fluorescence imaging, the cells were washed with cold PBS (4 °C) twice and fixed in cold 4% paraformaldehyde/PBS solution for 10 min. For the control experiment of single GFP molecule imaged on coverslip, GFP protein purified from *Escherichia coli* was firstly dissolved in the high salt buffer (600 mM NaCl, 150 mM PBS buffer, pH 7.4) to prevent the dimer formation and then immobilized on the coverslips through biotin coupled GFP antibody (Clontech) as previously reported [15].

For analysis of single-molecule fluorescence intensity in a movie acquired from living cells, the background fluorescence

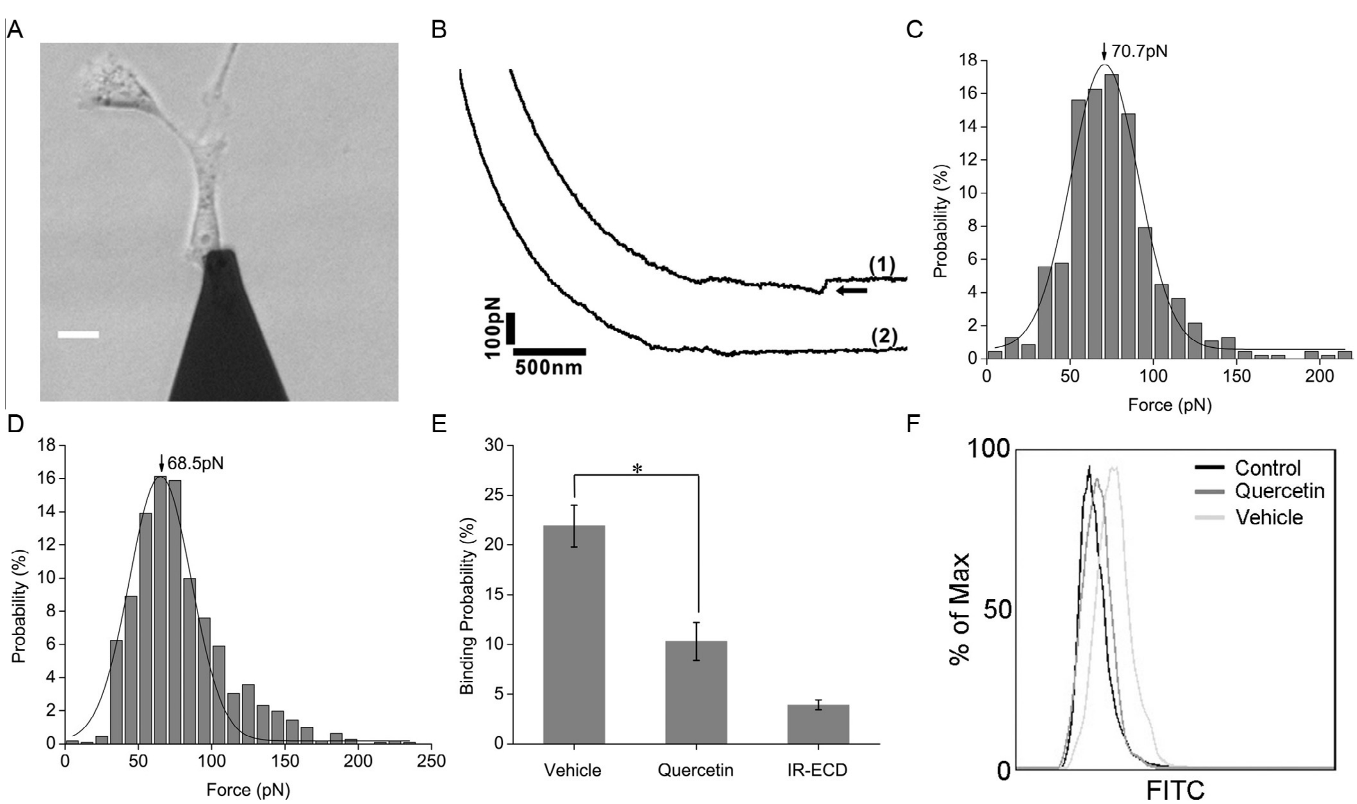

Fig. 1. Effect of quercetin on the interaction between insulin and IR. (A) An illuminated image of binding force measurements on MDA-MB-231 cells. Scale bar: 20 μM. (B) Representative force curves obtained with insulin-modified (1) or unmodified (2) AFM tips. (C and D) Histograms of binding forces of insulin/IR with the cells treated with 0.1% DMSO (vehicle) (C) or 100 μM quercetin (D) (gray bars, experimental data; solid line, theoretical Gaussian distribution curves). (E) The binding probability of insulin and IR when the cells are treated with vehicle, 100 μM quercetin or the blocking reagent (IR extracellular domain, IR-ECD). (F) Fluorescence intensity by flow cytometry using biotinylated insulin and avidin-FITC. The cells were treated with vehicle, quercetin (100 μM) or negative control reagent. *$P < 0.05$. Data is expressed as mean ± SEM.

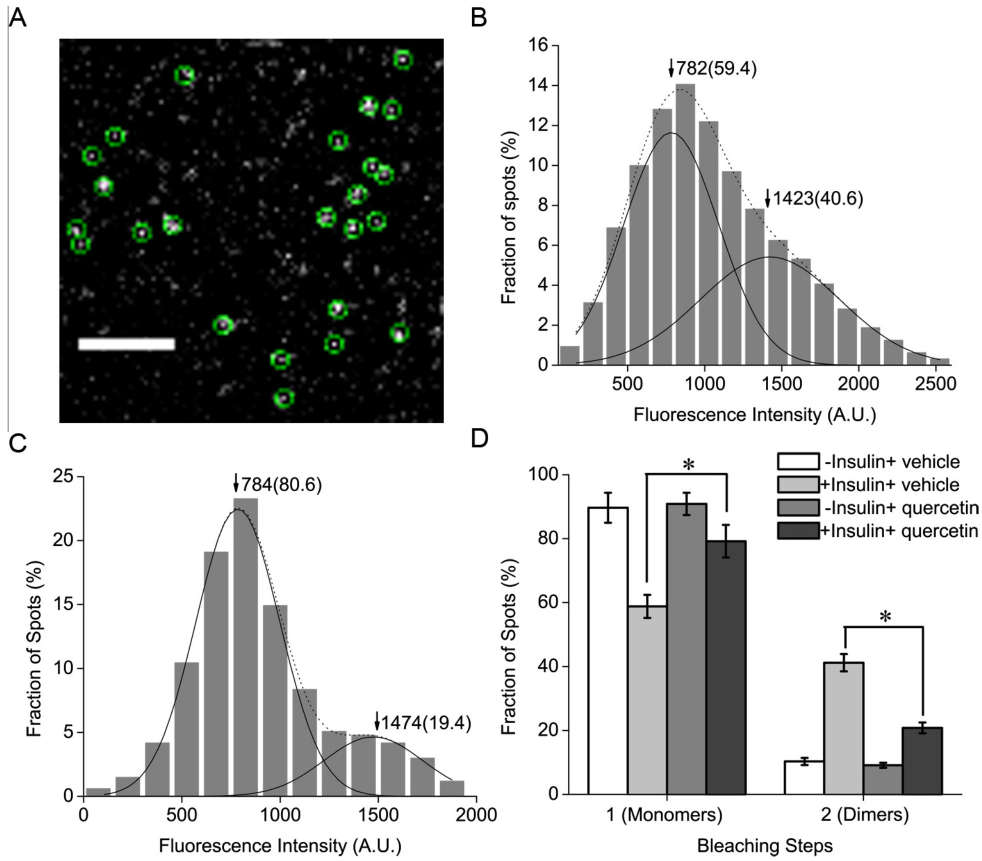

Fig. 2. Effect of quercetin on insulin induced IR dimerization. (A) A typical single-molecule image of IR-GFP on MDA-MB-231 cell membrane. The spots enclosed with green circles represented the signals from individual IR-GFP molecules. Scale bar: 4 μM. (B and C) Distributions of the fluorescence intensity of individual IR-GFP spots from the stimulated cells with 0.1% DMSO (vehicle) (B) or 100 μM quercetin (C) treatment. For insulin stimulation experiment, the transfected cells were incubated with 100 nM insulin in the serum-free DMEM for 30 min at 37 °C. The solid curves show the fitting of the Gaussian function with the arrowheads indicating the peak positions. The two peaks represented monomers and dimers, respectively, and the numbers in the parentheses are the fractions. (D) Frequency of one- and two-step bleaching events under various conditions. $^*P < 0.05$. Data is expressed as mean ± SEM. (For interpretation of the references to color in this figure legend, the reader is referred to the web version of this article.)

was first subtracted from each frame using the rolling ball method in Image J software (National Institute of Health). Then the first frame of each movie was used for fluorescent spot (regions of interest) selection. The image was thresholded (four times of the mean intensity of an area with no fluorescent spots), then filtered again with a user-defined program in Matlab. To analyze the photobleaching steps, regions of interest for bleaching analysis were selected according to the method previously reported [16]. The background fluorescence was subtracted from the movie acquired from the fixed cells using the rolling ball method in Image J software.

2.5. Western blotting

Western blotting was performed in order to study the downstream signaling of the IR pathway [17]. MDA-MB-231 cells were treated with vehicle (0.1% DMSO) or quercetin (100μM) for 30 min in the absence or presence of insulin. Cells were resuspended in 200 μl of 0.9% saline with protease inhibitors (1 mM phenylmethylsulfonyl fluoride, 10 μg/ml aprotinin, 10 μg/ml leupeptin, and 10 μg/ml pepstatin A) and mixed with 200 μl double-strength Laemmli buffer (100 mM Tris–HCl, pH 6.8, 200 mM dithiothreitol, 4% SDS, 0.2% bromophenol blue, and 20% glycerol). Cell lysates were denatured for 10 min at 95 °C. Cell lysates were separated by SDS gel electrophoresis (7.5% SDS gels) and transferred to polyvinylidene fluoride (PVDF membranes) with 0.192 M glycine, 0.025 M Tris and 10% methanol. Membranes were saturated for one hour at 4 °C in TBS, pH 7.4, containing 5% nonfat milk and probed for two hours at room temperature with primary antibodies for IR, p-IR, Akt and p-Akt (1:1000) (Cell Signaling). After washing the blots were probed for one hour at room temperature with peroxidase-conjugated secondary antibodies (1:3000). Antibody binding was detected by enhanced chemiluminescence (Amersham Life Sciences, Amersham, UK).

2.6. Glucose uptake assay

MDA-MB-231 cells were seeded in 96-well plates (1×10^4 cells/well) for 24 h, washed with phosphate-buffered saline (PBS) and incubated for 24 h with serum free media. Cells were thereafter treated with 0.1% dimethyl sulfoxide (DMSO) (vehicle) or quercetin (100 μM) for 1 h, followed by a 30-min incubation with 100 nM of insulin. Glucose uptake was measured using a glucose uptake cell-based assay kit (Cayman) according to the manufacturer's instructions. Three replicates were used for each group, and the experiments were repeated three times to confirm the results.

2.7. Cell proliferation assay

MDA-MB-231 cells were seeded in 96-well plates (1×10^4 cells/well) with complete medium for 24 h, followed by treatment with vehicle (0.1% DMSO) or 100 μM of quercetin for 24 h. Cellular

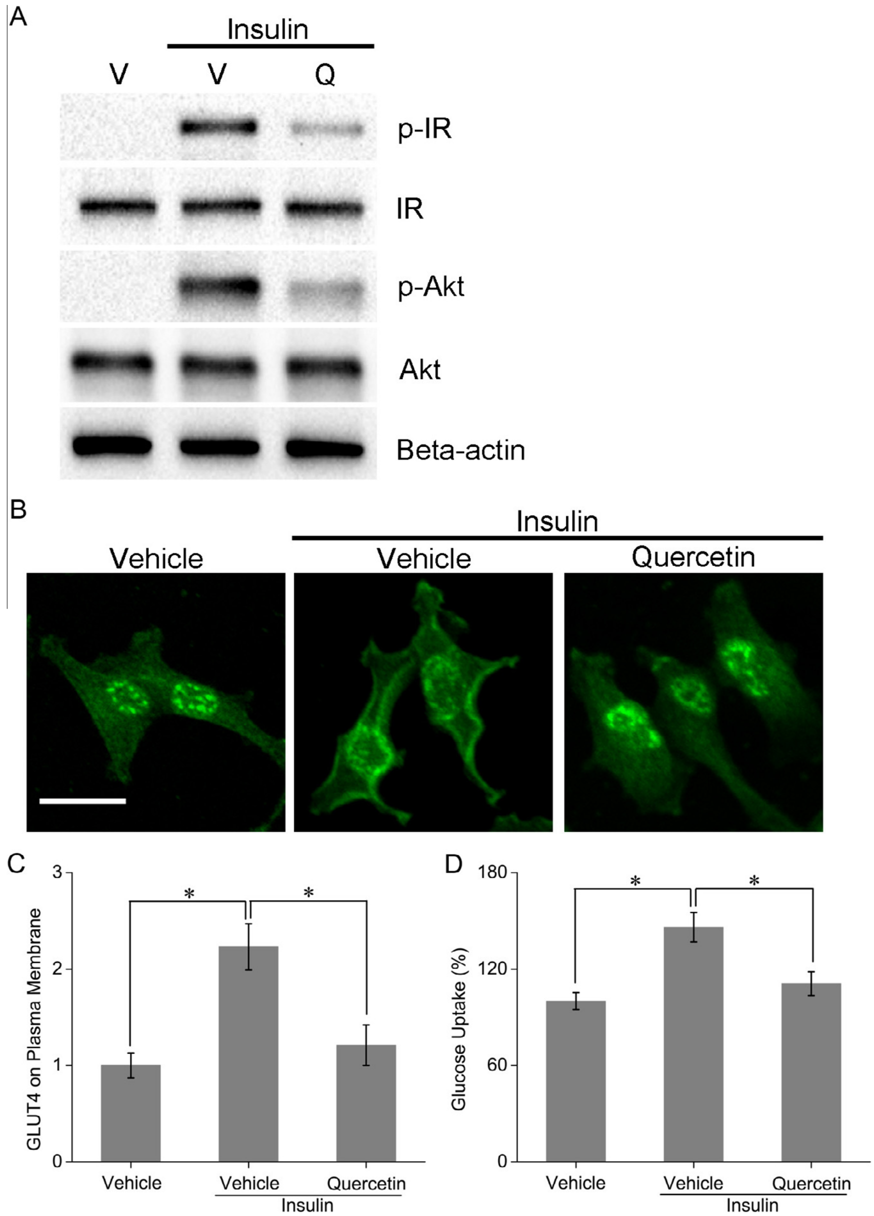

Fig. 3. Evaluation of quercetin on insulin receptor signaling. (A) Western blot analysis of phosphorylated insulin receptor (p-IR), phosphorylated Akt (p-Akt), insulin receptor (IR) and Akt. Cells were pretreated with 0.1% DMSO (vehicle, V) or 100 μM quercetin (Q) and stimulated with insulin for 30 min. (B) Confocal images of immunofluorescent detection of GLUT4. Cells were treated with vehicle (0.1% DMSO) or 100 μM quercetin and then incubated in the absence or presence of insulin. Scale bar, 20 μM. (C) Fluorescent intensity analysis of GLUT4 associated with the plasma membrane. In each group five cells were analyzed. Data are expressed as the mean fold change in fluorescent intensity (compared with the vehicle group). (D) MDA-MB-231 Cells were treated with vehicle or 100 μM quercetin in the absence or presence of insulin (100 nM). Glucose uptake assay was performed using a glucose uptake cell-based assay kit. $^{*}P < 0.05$. The results are expressed as the mean ± SEM.

proliferation was quantified using the CellTiter 96® AQueous Non-Radioactive Cell Proliferation Assay (Promega Corporation), according to the manufacturer's instructions.

2.8. Tumor model

All animal experiments were performed in compliance with guidelines of the Animal Welfare Act and the guide for the care and use of laboratory animals following protocols approved by the Institutional Animal Care and Use Committee (IACUC). MDA-MB-231 cells were mixed with 40% growth factor reduced matrigel and injected the mammary fat pad of female nude mice (Charles River, 4–6 weeks of age, 2×10^6 cells/mouse) to initiate tumor growth. The animals were randomly divided in two groups ($n = 6$). The first group received only 0.2 ml of vehicle by gavage daily and served as a control group. The second group of animals received 50 μg/mouse/day doses of quercetin in vehicle, respectively, for 4 weeks. Vehicle and quercetin feeding was started 2 weeks after cell inoculation and was continued for 4 weeks. Tumor sizes were measured twice weekly in two dimensions with calipers. Tumor volume (V, mm^3) was determined with the equation: $V = 0.5 \times \text{length} \times \text{width} \times \text{width}$ [18]. The tumor volume measurements were performed by an investigator who was unaware of the treatment groups.

2.9. Statistical analysis

T-test comparisons (two-tailed, unpaired) were performed to evaluate statistical significance.

3. Results and discussion

3.1. Insulin ligand–receptor interaction

To examine whether quercetin affects ligand-receptor interactions we performed single-molecule force spectroscopy in living MDA-MB-231cells, measuring the binding force and binding probability of insulin and insulin receptor (IR). To directly probe the binding force of insulin to IR, the tip of atomic force microscopy (AFM) was modified with insulin and moved to the cells which expressed IR (Fig. 1A). The rupture forces were detected when the tip and cell were brought into and out of contact (Fig. 1B) [19]. Blocking of the force with IR extracellular domain (IR-ECD) was carried out to confirm the measured forces were the specific ones between insulin and IR. The force distribution histogram displayed a single maximum by a Gaussian fit, indicating that the single-molecule forces were measured. The low frequency of the adhesion events during the measurement also ensured that the force was mediated by a single ligand-receptor pair (<25% adhesion events ensured >90% probability of single-molecule force measurement). Although the rupture force that the ligand binds to the receptor is similar to that of the control (Fig. 1C and D), quercetin treatment lowers the binding probability (control: 21.9% ± 2.1%, quercetin: 10.3% ± 1.9%) (Fig. 1E). To further confirm that quercetin blocks the binding between the ligand–receptor pair, flow cytometry was performed using biotinylated insulin and avidin-FITC. We found that the fluorescence signal decreased in the presence of quercetin (Fig. 1F).

3.2. Insulin receptor dimerization

Previous report has been shown that the IRs exist as monomers at low expression levels, and follow the general ligand–induced receptor dimerization model for activation upon insulin stimulation [8,20]. Here we used single-molecule fluorescence microscopy to examine the effect of quercetin on the formation of insulin induced IR dimerization, which is a prerequisite for IR phosphorylation and signal propagation. As shown in the typical TIRFM image of resting MDA-MB-231 cells (Fig. 2A and Supplementary Video 1), IR-GFP molecules appeared as well-dispersed diffraction-limited fluorescent spots (5×5 pixels, 800×800 nM). The fluorescence intensities of these spots maintained mostly for less than 4.5 s and then suddenly dropped to the background level, indicating that they are single IR molecules. The fluorescence intensity distribution of the spots exhibited a sum of two Gaussian distributions (Fig. S1A). While the first population of IR monomers had a peak intensity close to that of single GFP molecules on the glass coverslips (Fig. S1C), the second population of IR dimers had a peak value about twice of the first one. With 312 counted spots, 89.3% were monomers and 10.7% were dimers. After insulin stimulation, the population of monomers decreased to 59.4% and that of dimers increased to 40.6% (Fig. 2B). Then we treated the cells with quercetin before fluorescence imaging. The fluorescence intensity distribution of the spots from the cells was very similar to that obtained in the cells without quercetin treatment (with 356 counted spots, monomers 90.9% and dimers 9.1%) (Fig. S1B). However, after insulin stimulation, the fluorescence intensity distribution (with 335 spots counted monomers 80.6% and dimers 19.4%) obtained from quercetin cells was significantly different from that obtained with the untreated cells (Fig. 2C). The population of IR dimers decreased from 40.6% to 19.4% for quercetin treated cells. This indicated that quercetin inhibited ligand–induced IR dimerization. The bleaching-step counting method is considered as an alternative way to examine dimer formation, where one-step photobleaching spots represent monomers and two-step spots represent dimers (Fig. S2). Using this technique, we obtained the similar results that the population of two-step photobleaching spots, which represent dimers, decreased from 41.2 ± 2.7% to 20.8 ± 1.6% after quercetin treatment for the stimulated cells (Fig. 2D).

3.3. Insulin receptor downstream signaling

To confirm the inhibitory effect of quercetin on insulin receptor signaling pathway, we investigate phosphorylation of IR and Akt. The result shows that quercetin effectively inhibits the insulin induced phosphorylation of IR and Akt in MDA-MB-231 cells (Fig. 3A). It is known that insulin stimulated activation of Akt is able to translocate GLUT4 to the cell membrane, causing an increased glucose uptake [21]. Our data reveals that treatment with quercetin significantly inhibits GLUT4 membrane translocation and impairs glucose uptake in response to insulin (Fig. 3B–D).

3.4. Cell proliferation and tumor growth

Because quercetin inhibits both insulin stimulated activation of insulin receptor signaling and glucose uptake, which promotes cell proliferation [22–24], we investigated the effect of quercetin on insulin stimulated cell proliferation. The results indicate that quercetin inhibited insulin induced cell proliferation (Fig. 4A). Furthermore, we evaluated the effect of quercetin on MDA-MB-231 breast tumor growth in nude mice. Quercetin administration caused a significant decrease in tumor growth compared to the

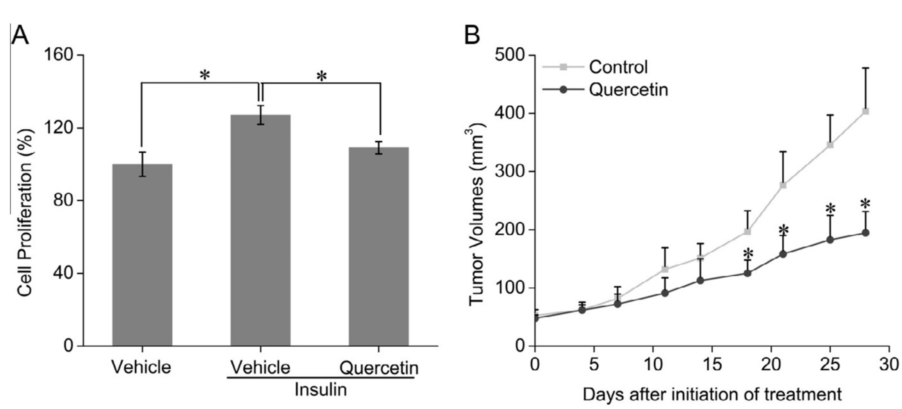

Fig. 4. Evaluation of quercetin on cell proliferation and tumor growth. (A) MDA-MB-231 cells were incubated with serum-free medium and treated with 0.1% DMSO (vehicle) or 100 μM quercetin in the presence of insulin. (B) Mice with MDA-MB-231 tumors were treated with oral administration of the vehicle or 50 μg quercetin. Statistical comparisons were made between the quercetin group and the vehicle group. $^*P < 0.05$. The results are expressed as the mean ± SEM.

control group, lending further support to the ability of quercetin in inhibiting cancer cell proliferation (Fig. 4B).

In summary, we have employed single-molecule force spectroscopy and fluorescence microscopy to study the inhibition mechanism of quercetin on insulin receptor signaling in living cells. Our results demonstrated that quercetin reduced the binding probability of insulin to its receptor IR, thus inhibited the receptor dimerization and activation for the signaling complex formation and the subsequent Akt phosphorylation for the downstream signal transduction. Quercetin was also found to suppress insulin induced GLUT4 membrane translocation, resulting in decreased glucose uptake and impaired proliferation. Furthermore, our *in vivo* experiments showed that quercetin intake significantly inhibits tumor growth. Therefore, quercetin may be worthy of further development as an anticancer agent, exploiting its effectiveness in inhibiting insulin receptor signaling for cancer therapy. Our study also provides a new approach of applying single-molecule techniques to identify the chemical compounds for cell signaling inhibition.

Acknowledgments

The authors acknowledge supports from the following funding source: Excellent Academic Backbone Program of Tenth People's Hospital of Shanghai (No. 12XSGG102).

Appendix A. Supplementary data

Supplementary data associated with this article can be found, in the online version, at http://dx.doi.org/10.1016/j.bbrc.2014.09.039.

References

[1] J. Nakae, Y. Kido, D. Accili, Distinct and overlapping functions of insulin and IGF-I receptors, Endocr. Rev. 22 (2001) 818–835.
[2] S.D. Narasimhan, K. Yen, H.A. Tissenbaum, Converging pathways in lifespan regulation, Curr. Biol. 19 (2009) R657–R666.
[3] K. Siddle, Signalling by insulin and IGF receptors: supporting acts and new players, J. Mol. Endocrinol. 47 (2011) R1–R10.
[4] A. Belfiore, F. Frasca, G. Pandini, L. Sciacca, R. Vigneri, Insulin receptor isoforms and insulin receptor/insulin-like growth factor receptor hybrids in physiology and disease, Endocr. Rev. 30 (2009) 586–623.
[5] K.D. Burroughs, S.E. Dunn, J.C. Barrett, J.A. Taylor, Insulin-like growth factor-I: a key regulator of human cancer risk?, J Natl. Cancer Inst. 91 (1999) 579–581.
[6] M. Pollak, Insulin and insulin-like growth factor signalling in neoplasia, Nat. Rev. Cancer 8 (2008) 915–928.
[7] V.N. Anisimov, Insulin/IGF-1 signaling pathway driving aging and cancer as a target for pharmacological intervention, Exp. Gerontol. 38 (2003) 1041–1049.
[8] K. Baer, H. Al-Hasani, S. Parvaresch, T. Corona, A. Rufer, V. Nolle, E. Bergschneider, H.W. Klein, Dimerization-induced activation of soluble insulin/IGF-1 receptor kinases: an alternative mechanism of activation, Biochemistry 40 (2001) 14268–14278.
[9] V.V. Kiselyov, S. Versteyhe, L. Gauguin, P. De Meyts, Harmonic oscillator model of the insulin and IGF1 receptors' allosteric binding and activation, Mol. Syst. Biol. 5 (2009) 243.
[10] C.W. Ward, M.C. Lawrence, Ligand-induced activation of the insulin receptor: a multi-step process involving structural changes in both the ligand and the receptor, BioEssays 31 (2009) 422–434.
[11] M. Nomura, T. Takahashi, N. Nagata, K. Tsutsumi, S. Kobayashi, T. Akiba, K. Yokogawa, S. Moritani, K. Miyamoto, Inhibitory mechanisms of flavonoids on insulin-stimulated glucose uptake in MC3T3-G2/PA6 adipose cells, Biol. Pharm. Bull. 31 (2008) 1403–1409.
[12] X.S. Xie, J.K. Trautman, Optical studies of single molecules at room temperature, Annu. Rev. Phys. Chem. 49 (1998) 441–480.
[13] P.A. Hoyne, L.J. Cosgrove, N.M. McKern, J.D. Bentley, N. Ivancic, T.C. Elleman, C.W. Ward, High affinity insulin binding by soluble insulin receptor extracellular domain fused to a leucine zipper, FEBS Lett. 479 (2000) 15–18.
[14] Y. Yang, J. Wolfram, X. Fang, H. Shen, M. Ferrari, Polyarginine induces an antitumor immune response through binding to toll-like receptor 4, Small 10 (2014) 1250–1254.
[15] Y. Yang, J. Wolfram, J. Shen, Y. Zhao, X. Fang, H. Shen, M. Ferrari, Live-cell single-molecule imaging reveals clathrin and caveolin-1 dependent docking of SMAD4 at the cell membrane, FEBS Lett. 587 (2013) 3912–3920.
[16] M.H. Ulbrich, E.Y. Isacoff, Subunit counting in membrane-bound proteins, Nat. Methods 4 (2007) 319–321.
[17] Y. Yang, J. Wolfram, H. Shen, X. Fang, M. Ferrari, Hesperetin: an inhibitor of the transforming growth factor-beta (TGF-beta) signaling pathway, Eur. J. Med. Chem. 58 (2012) 390–395.
[18] F. Wang, Y. Yang, Suppression of the xCT-CD44v antiporter system sensitizes triple-negative breast cancer cells to doxorubicin, Breast Cancer Res. Treat. (2014).
[19] J. Yu, Q. Wang, X. Shi, X. Ma, H. Yang, Y.G. Chen, X. Fang, Single-molecule force spectroscopy study of interaction between transforming growth factor beta1 and its receptor in living cells, J. Phys. Chem. B 111 (2007) 13619–13625.
[20] N.M. McKern, M.C. Lawrence, V.A. Streltsov, M.Z. Lou, T.E. Adams, G.O. Lovrecz, T.C. Elleman, K.M. Richards, J.D. Bentley, P.A. Pilling, P.A. Hoyne, K.A. Cartledge, T.M. Pham, J.L. Lewis, S.E. Sankovich, V. Stoichevska, E. Da Silva, C.P. Robinson, M.J. Frenkel, L.G. Sparrow, R.T. Fernley, V.C. Epa, C.W. Ward, Structure of the insulin receptor ectodomain reveals a folded-over conformation, Nature 443 (2006) 218–221.
[21] G. Sweeney, R.R. Garg, R.B. Ceddia, D. Li, M. Ishiki, R. Somwar, L.J. Foster, P.O. Neilsen, G.D. Prestwich, A. Rudich, A. Klip, Intracellular delivery of phosphatidylinositol (3,4,5)-trisphosphate causes incorporation of glucose transporter 4 into the plasma membrane of muscle and fat cells without increasing glucose uptake, J. Biol. Chem. 279 (2004) 32233–32242.
[22] A. Singh, A. Purohit, H.A. Hejaz, B.V. Potter, M.J. Reed, Inhibition of deoxyglucose uptake in MCF-7 breast cancer cells by 2-methoxyestrone and 2-methoxyestrone-3-O-sulfamate, Mol. Cell. Endocrinol. 160 (2000) 61–66.
[23] M. Okumura, M. Yamamoto, H. Sakuma, T. Kojima, T. Maruyama, M. Jamali, D.R. Cooper, K. Yasuda, Leptin and high glucose stimulate cell proliferation in MCF-7 human breast cancer cells: reciprocal involvement of PKC-alpha and PPAR expression, Biochim. Biophys. Acta 1592 (2002) 107–116.
[24] A.W. Harmon, Y.M. Patel, Naringenin inhibits glucose uptake in MCF-7 breast cancer cells: a mechanism for impaired cellular proliferation, Breast Cancer Res. Treat. 85 (2004) 103–110.